Hydrogen site occupancy and hydrogen diffusion in $LaNi_4BH_{1.5}$

F. E. Spada* and H. Oesterreicher
Chemistry Department, University of California—San Diego, La Jolla, California 92093

R. C. Bowman, Jr. and M. P. Guse
Monsanto Research Corporation—Mound, Miamisburg, Ohio 45342

(Received 14 September 1983; revised manuscript received 13 April 1984)

The $CeCo_4B$-type ternary compound $LaNi_4B$ reacts with hydrogen gas at room temperature to form the hydride $LaNi_4BH_{1.5}$ in the pressure range 1—100 atm. Rigid-lattice proton second moments indicate that hydrogen only occupies sites within the La-Ni basal planes in this hydride. The La-B planes, which do not accommodate hydrogen, appear to act as barriers to long-range hydrogen diffusion along the [001] direction. We have studied the diffusion behavior of hydrogen in $LaNi_4BH_{1.4}$ by NMR measurements of the proton relaxation times T_1 and $T_{1\rho}$ and find evidence for at least two activated-jump processes. The long-range diffusion process is characterized by lower mobilities and larger activation energies than observed in $LaNi_5H_6$; comparison of the results with those previously obtained for $LaNi_4AlH_{4.3}$ suggests that the activated step for diffusion in these hydrides is passage of hydrogen through the $12o$ sites, or through saddle points joining these sites to other sites occupied by hydrogen. Evidence for a low-activation-energy process is also observed; this process is interpreted as a localized hopping within clusters of $3f$-$12n$ sites that does not result in hydrogen transport. These observations are consistent with the five-site model [$P6/mmm$ (D^1_{6h}) space group] for hydrogen site occupancy in $LaNi_5H_6$, but they are less easily related to site occupancies for the $P31m$ (C^2_{3v}) model. Additionally, the presence of several anomalies in the $LaNi_4B$ x-ray powder pattern prompted us to conduct single-crystal investigations which indicate that the $CeCo_4B$ structure represents only a subcell in a larger hexagonal antiphase domain structure extending along the directions of the basal-plane axes.

I. INTRODUCTION

Recently several proton NMR investigations of hydrogen diffusion in β-$LaNi_5H_6$ (Refs. 1—3) and β-$LaNi_{5-x}Al_xH_z$ (Refs. 4 and 5) ($0 \le x \le 1.5$) have been conducted in an effort to understand the microscopic nature of hydrogen motion in $CaCu_5$-type hydrides. It is now apparent that hydrogen motion in these hydrides proceeds via a complex mechanism, with evidence existing for at least two activated-jump processes.[3,5] It has also been established that the diffusion activation energy E_a increases with x in the aluminum-substituted hydrides, resulting in substantially reduced hydrogen mobility.[4] Since aluminum exclusively replaces the nickel atoms in the $3g$ sites,[6] Bowman and co-workers[5] have suggested that the presence of aluminum in these sites may restrict the low-energy diffusion pathways and therefore decouple the low- and high-energy processes. Further elaboration on the changes in the hydrogen diffusion mechanism caused by aluminum substitution has not been possible because two quite different models for deuterium site occupancy in β-$LaNi_5D_6$ have been proposed.[6–9]

The hydride of the ternary boride $LaNi_4B$ presents new opportunities to gain additional insights into the mechanism of hydrogen diffusion in $CaCu_5$-type systems. $LaNi_4B$ has been reported[10] to crystallize with the $CeCo_4B$ structure,[11] which is derived from the $CaCu_5$ structure by completely substituting boron for the $2c$ transition metal in alternating layers perpendicular to the [001] direction. As illustrated in Fig. 1, this results in a doubled $CaCu_5$ atomic arrangement belonging to the $P6/mmm$ space group with two inequivalent rare-earth sites ($1a$ and $1b$), two types of transition-metal sites ($2c$

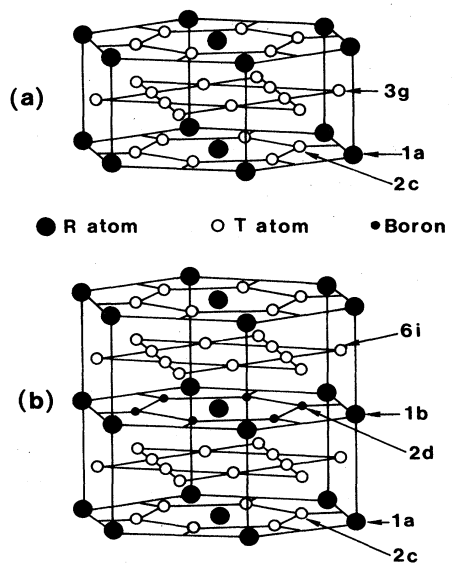

FIG. 1. Comparison of the $CaCu_5$ and $CeCo_4B$ structures. R denotes rare earth; T denotes transition metal. Wyckoff labels for the different metal atom positions are indicated. (a) $CaCu_5$ structure and (b) $CeCo_4B$ structure; the $6i$ transition-metal planes are displaced towards the R-B layer ($z = 0.287$).

and 6*i*), and one type of boron site (2*d*). It should be noted that the 6*i* transition-metal layers in $CeCo_4B$-type materials are slightly displaced towards the rare-earth—boron midplane ($z=0.287$).[11] The crystallographic features of the $CeCo_4B$ structure suggested to us that a study of hydrogen diffusion in $LaNi_4B$ hydride should expand and complement previous studies on β-$LaNi_{5-x}Al_xH_z$,[4,5] where only the 3*g* transition-metal sites were influenced by aluminum substitution.

We have investigated the hydrogen absorption characteristics of $LaNi_4B$ and have found that it forms the hydride $LaNi_4BH_{1.5}$. We have also studied the diffusion behavior and site occupancy of hydrogen in this hydride by measuring the T_1 and $T_{1\rho}$ proton NMR relaxation times and the proton rigid-lattice second moment (M_2). In the course of these studies we have found that the $CeCo_4B$ atomic arrangement does not completely describe the $LaNi_4B$ structure, but instead represents only a subcell in a larger superstructure. The results of these investigations are presented in this report and are used with the results of previous measurements on β-$LaNi_{5-x}Al_xH_z$ to discuss possible hydrogen diffusion mechanisms in β-$LaNi_5H_6$ and related systems.

II. EXPERIMENTAL DETAILS

A. Intermetallic preparation and characterization

The ternary compound $LaNi_4B$ was prepared by arc melting stoichiometric quantities of 99.99% pure lanthanum (Rare Earth Products, Ltd., England), 99.998+% pure nickel (Koch-Light Laboratories, Ltd., England), and 99.9% pure boron (Atomergic Chemetals, New York) on a water-cooled copper hearth under an argon atmosphere. Because the properties of $LaNi_5$ and its hydride are well known, a specimen of $LaNi_5$ was also prepared from the same lanthanum and nickel stocks and used as a reference material in these studies. In the case of $LaNi_4B$, nickel and boron were first melted together followed by the addition of lanthanum to the nickel-boron pellet. The sample ingots were turned over and remelted several times to ensure homogeneous compositions. Final sample stoichiometries were determined by reweighing after the melt. X-ray powder patterns obtained with Cu $K\alpha$ radiation were used to verify the phase purity of each intermetallic. Annealed specimens were wrapped in tantalum foil and sealed in quartz tubes under argon prior to heat treatment.

Immediately prior to hydriding, the $LaNi_4B$ and $LaNi_5$ samples employed for the NMR studies were pulverized and sieved (particle size $\lesssim 74$ μm) in a glove bag flushed with helium gas. Pulverization minimizes skin-effect problems which limit the penetration depth of rf fields into metallic conductors, but it also results in larger amounts of surface nickel in $LaNi_5$ when the surface segregates into nickel and La_2O_3 because of the increased surface-to-volume ratio of the powder.[12–14] Samples of the powders, as well as bulk specimens, were therefore subjected to magnetic analysis using a vibrating sample magnetometer (Princeton Applied Research Corporation, New Jersey) in order to estimate the amount of free nickel present on the surface in each specimen.

B. Hydrogen composition measurements

The intermetallics were hydrided via direct reaction with hydrogen gas (99.995% purity; $[O_2]+[H_2O]\leq 6$ ppm). Hydrogen compositions were determined by monitoring pressures in a system having a known volume. Pressures in the range 10—100 atm were monitored with a strain gauge transducer (Viatran Corporation, New York) while pressures less than 10 atm were monitored with a capacitance manometer having a resolution of 1.3×10^{-4} atm (MKS Instruments, Massachusetts). Desorption isotherms were measured with the sample contained in a stainless-steel chamber which permitted sample temperatures to be monitored with a sheathed thermocouple in direct contact with the specimen. Pulverized samples for the NMR studies were hydrided inside the glass NMR tubes by exposure to 10—20 atm H_2 with the aid of a device which maintained zero differential pressure across the glass walls; after initial absorption was complete the hydrogen pressure was reduced to 1—2 atm, the sample was quenched to 77 K, and the glass tube was sealed with a flame. Elevated temperatures were achieved by immersing the sample chambers in a heated oil bath which was maintained constant to within ±1 K with a time-proportioning temperature controller (Omega Engineering, Connecticut).

C. NMR measurements

The proton relaxation times T_1 and $T_{1\rho}$ were measured at a resonance frequency of 34.5 MHz using conventional pulse sequences.[4,5] A spin-locking field of 7.3 G was employed for the $T_{1\rho}$ measurements. A simplified version of the magic-echo pulse sequence[15] was used to measure the proton line shapes at a resonance frequency of 56.4 MHz and at 78 K to ensure that rigid-lattice conditions were satisfied. The experimental second moments (M_2) were obtained from Gaussian plots of the initial portions of the proton dipolar echoes. The two transient NMR spectrometers used in this study have been described elsewhere,[16] and have different sample-tube requirements. Samples were sealed in 5-mm-o.d. glass tubes for the M_2 determinations and in 7-mm-o.d. glass tubes for the T_1 and $T_{1\rho}$ measurements.

III. RESULTS AND DISCUSSION

A. Crystallographic considerations

The ternary compound $LaNi_4B$ was quenched directly from the melt and was determined by weighing to have the composition $LaNi_{4.0}B_{1.0}$. Although the as-cast specimen produced an x-ray powder pattern that is very similar to the diffraction patterns of other materials crystallizing with the $CeCo_4B$ structure, indexing the pattern was made difficult by the presence of several anomalies. Annealing the sample at 1073 K for one week had no influence on the appearance of the powder pattern. The most obvious difference from $CeCo_4B$-type patterns is the presence of several low-intensity reflections forbidden by the $CeCo_4B$ structure. Furthermore, reflections corresponding to those allowed by this structure and having odd values for

the Miller index are slightly displaced from their expected positions. However, if the $CeCo_4B$ indices (220) and (004) are assigned to the diffraction peaks attributed to the interplanar spacings $d=1.279$ and 1.749 Å, respectively, one obtains the hexagonal lattice parameters $a_0'=5.118\pm0.006$ Å and $c_0'=6.997\pm0.012$ Å, which are in excellent agreement with previously reported $LaNi_4B$ cell constants.[17] Another problem with the observed $LaNi_4B$ x-ray pattern is that the reflection associated with the spacing $d=2.396$ Å has a significantly depressed intensity when compared to the corresponding (111) reflection in a theoretical $LaNi_4B$ pattern computed on the basis of the $CeCo_4B$ structure. We concluded from these observations that, contrary to previous reports,[10] the $CeCo_4B$ structure does not completely describe the true $LaNi_4B$ atomic arrangement.

Single-crystal studies of the $LaNi_4B$ structure were undertaken to investigate the origin of the anomalies in the powder pattern. A report of these studies will be presented elsewhere, but we will mention that the single-crystal results indicate that the $CeCo_4B$ atomic arrangement represents only a subcell in a larger superstructure extending along the [100] direction. Precession photographs of the $LaNi_4B$ reciprocal lattice reveal that the true $LaNi_4B$ structure is hexagonal with lattice parameters $a_0=30.71\pm0.10$ Å and $c_0=6.995\pm0.012$ Å. Each primary reflection in *hkl* reciprocal-lattice layers with odd *l* has negligible intensity and is replaced by a cluster of weak satellite reflections which surround the position of the absent primary spot. Reciprocal-lattice layers with even *l* show only the strong primary reflections separated by distances corresponding to the subcell lattice parameters $a_0'=5.118\pm0.017$ Å. The lattice parameters of the $CeCo_4B$-type subcell are therefore related to the true unit cell by the relations $a_0=6a_0'$ and $c_0=c_0'$. These observations are consistent with the results of other single-crystal studies which reported the existence of superstructures in the related ternary borides YNi_4B ($a_0=3a_0'$) (Ref. 18) and $CeNi_4B$ ($a_0=8a_0'$) (Ref. 19).

Reciprocal lattices having satellite spots such as those described here are typical of materials having long-period superlattices.[20] This special group of superlattices is characterized by periodic antiphase domain structures in which subcells of adjacent domains are related to one another by a lattice shift. The observation that satellite reflections are present only in reciprocal-lattice layers having odd *l* suggests that the out-of-phase step at the antiphase boundary is a shift of $c_0/2$ along the [001] direction. The long-period superstructure therefore can be envisioned as resulting from nickel and boron atoms periodically exchanging positions between the (001) and (002) planes in a group of $CeCo_4B$-type subcells.

The $LaNi_5$ specimen was quenched from the melt and produced an x-ray diffraction pattern with reflections corresponding only to this intermetallic. Comparison of the measured lattice parameters $a_0=5.014\pm0.004$ Å and $c_0=3.979\pm0.008$ Å with published values[21,22] indicated a stoichiometry of $LaNi_{5.0}$, in agreement with a determination based on weighing after the melt. The quenched $LaNi_5$ specimen was not subjected to annealing treatments prior to hydriding.

B. Magnetic behavior of unhydrided materials

It is well known that the surface of $LaNi_5$ decomposes into elemental nickel and La_2O_3 when the intermetallic is exposed to trace amounts of O_2.[12,13] Karlicek and Lowe[3] have reported that the presence of surface nickel in $LaNi_5H_6$ influences the values of the proton relaxation times in this hydride. In particular, they observed excessive inhomogeneous broadening of the NMR line shapes as well as shifts of the $T_{1\rho}$ minimum to lower temperatures and anomalous short $T_{1\rho}$ values below this minimum when free nickel was present. By measuring the magnetic properties of the intermetallic prior to hydriding, we have attempted to characterize the extent of surface segregation caused by our sample handling techniques.

The magnetic behavior of bulk and pulverized specimens of both $LaNi_4B$ and $LaNi_5$ are summarized in Fig. 2, where the dependences of the sample magnetization (M) on temperature and the applied magnetic field (H_a) are shown. Bulk specimens of $LaNi_4B$ and $LaNi_5$ both displayed Pauli paramagnetic behavior. The former exhibited a constant magnetization of 2 emu/mole between

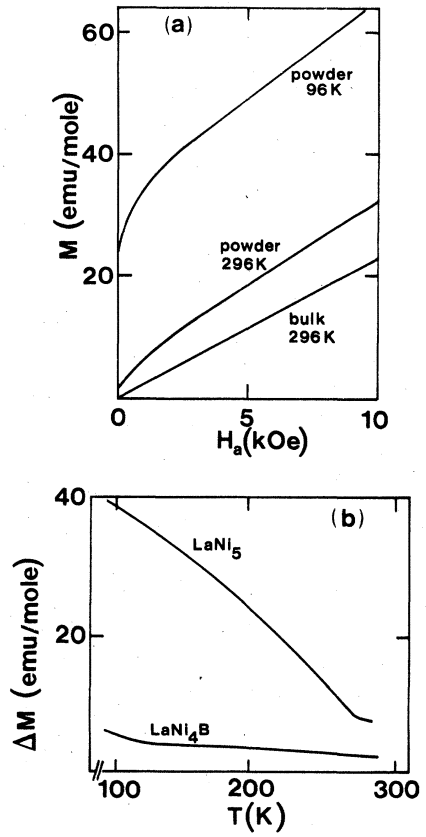

FIG. 2. Magnetic behavior of unhydrided $LaNi_5$ and $LaNi_4B$. (a) M-vs-H_a curves for bulk and pulverized $LaNi_5$ specimens. (b) ΔM-vs-T curves for pulverized $LaNi_5$ and $LaNi_4B$ specimens; ΔM is the magnetization of the powder corrected for the paramagnetism of the bulk.

90 K and room temperature in an applied field of 7.2 kOe ($\chi = 7.2 \times 10^{-7}$ emu/g), while the magnetization of the latter decreased slightly from 21 emu/mole at 90 K to 17 emu/mole at room temperature in the same field ($\chi = 5.5 \times 10^{-6}$ emu/g). Pulverization resulted in increased magnetizations for both intermetallics. In a 7.2-kOe applied field, M varied from 58 to 25 emu/mole between 90 and 295 K for pulverized $LaNi_5$, and it varied from 8.6 to 4.9 emu/mole in the same temperature range for $LaNi_4B$ powder. The field dependence of the magnetization for pulverized $LaNi_5$ shown in Fig. 2(a) indicates that a paramagnetic component is superimposed on a ferromagnetic component which saturates at about 2 kOe. We did not investigate the M-versus-H_a behavior of $LaNi_4B$ because of the small values of magnetization.

The magnetic behavior of the pulverized $LaNi_5$ sample is characteristic of the superparamagnetic and ferromagnetic nickel clusters which form on the surface of $LaNi_5$ when surface segregation occurs.[13(b),14] The 96-K M-versus-H_a curve for pulverized $LaNi_5$ extrapolates to a magnetization of 32 emu/mole at zero field. If this value is assumed to result entirely from elemental nickel, it indicates that 0.2% of the total available nickel is in the ferromagnetic state. This amount is in general agreement with the values 0.4—1.6% reported for 5-μm $LaNi_5$ particles.[14] The extrapolated value may also be used together with Fig. 7 of Ref. 13(a) to deduce that this magnetization is equivalent to that found in a $LaNi_5$ specimen exposed to 10—30 complete hydrogenation-dehydrogenation cycles. The difference in magnetization between bulk and pulverized $LaNi_4B$ [Fig. 2(b)] suggests that surface segregation is also occurring in this intermetallic and, by using the bulk-corrected magnetization 6.6 emu/mole (90 K, 7.2 kOe) as an upper limit for M, we estimate that 0.05% of the available nickel can be considered as free nickel in the pulverized $LaNi_4B$ specimen. This value is less than that found in similarly treated $LaNi_5$, but the specific nature and extent of decomposition in $LaNi_4B$ remain unknown because the possible existence of nonmagnetic species (e.g., $LaBO_3$ and La-Ni-B phases) cannot be ruled out by the present results.

The susceptibility of the quenched, bulk $LaNi_5$ specimen is about 12% larger than the value reported for $LaNi_{4.97}$.[13] This result, and the absence of ferromagnetic nickel in the bulk sample [Fig. 2(a)], may indicate that the $LaNi_5$ preparation of the present study has a superstoichiometric composition represented by $LaNi_{5+x}$ ($x < 0.1$), although the composition was determined to be $LaNi_{5.0}$ as mentioned in the preceding section. Single-phase specimens of $LaNi_{5+x}$ are easily prepared by quenching from above 1273 K, but annealing these superstoichiometric samples below 1173 K results in two-phase materials consisting of $LaNi_{5.0}$ and elemental nickel.[21] For this reason, the quenched $LaNi_5$ sample was not annealed. Excess nickel in single-phase $LaNi_{5+x}$ is accommodated as Ni-Ni pairs which replace some of the lanthanum atoms.[22] It is conceivable that such defects could influence the mechanism of hydrogen diffusion in $LaNi_5H_6$, but it is expected that the effects will be very small in the specimen prepared for this study because the defects should be very dilute.

C. Hydride formation

Desorption isotherms for $LaNi_4B$ hydride are presented in Fig. 3 and indicate that $LaNi_4B$ forms the hydride $LaNi_4BH_{1.5}$ in the pressure range 1—100 atm at room temperature. We also conducted a limited investigation at higher pressures using a previously described high-pressure hydriding manifold,[23] but no indication of a high-pressure plateau was observed up to 700 atm at 297 K. Under these latter conditions the maximum hydride composition was $LaNi_4BH_{1.8}$. The reaction of $LaNi_4B$ with hydrogen is characterized by slow kinetics. The sluggishness of the reaction was particularly evident at 273 K, where a minimum period of 15 h was required before equilibrium was achieved at each data point in the isotherm. X-ray diffraction patterns of $LaNi_4BH_z$ exhibit the same anomalies as observed in the powder patterns of the parent intermetallic and indicate that the hydrides retain the hexagonal structure. Only the a_0 parameter expands for $z \leq 1$, but for $z > 1$ both a_0 and c_0 expand. Lattice parameters for the $CeCo_4B$-type subcell, which were derived from the d values corresponding to the (220) and (004) reflections in $CeCo_4B$-type patterns, are listed in Table I.

The quenched $LaNi_5$ sample produced hydrogen desorption isotherms which are in excellent agreement with published isotherms. The characteristics of $LaNi_5H_6$ are thoroughly documented in the literature[24] and will not be described here.

Quite clearly, the hydrogen absorption properties of $LaNi_4B$ are substantially different from those of $LaNi_5$. The very small hydrogen capacity of $LaNi_4B$ suggests that hydrogen is excluded from sites near the La-B midplane and the 6i transition-metal layer (Fig. 1). Since sites within the La-Ni basal plane of $LaNi_4B$ have environments similar to those found in $LaNi_5$, it is reasonable to assume that hydrogen is accommodated in the interstitial

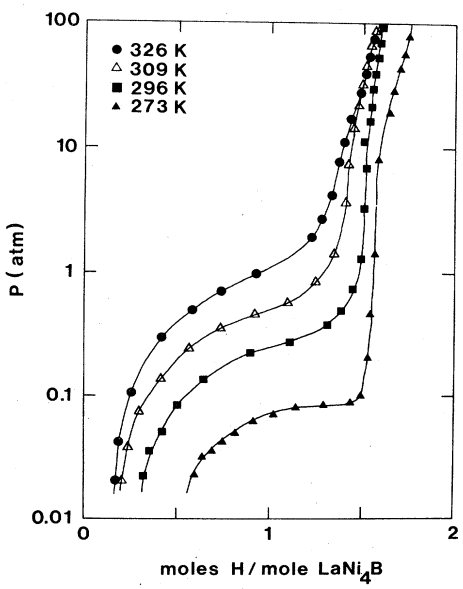

FIG. 3. Desorption isotherms for $LaNi_4B$ hydride.

TABLE I. Structural parameters for $LaNi_4BH_z$. Parameters correspond to the $CeCo_4B$-type subcell lattice constants.

Hydride Composition	a_0 (Å)	c_0 (Å)	c_0/a_0
$LaNi_4B$	5.118	6.997	1.37
$LaNi_4BH_{0.9}$	5.172	6.997	1.35
$LaNi_4BH_{1.4}$	5.234	7.085	1.35

sites in this plane. The x-ray data support this view since only the a_0 axis of the basal plane expands up to the composition of $LaNi_4BH_1$.

D. M_2 measurements and hydrogen site occupancy

When a metal hydride is cooled to a sufficiently low temperature hydrogen motion between different sites essentially ceases and the "rigid-lattice" limit for NMR phenomena is reached.[25] Under these conditions the dipolar interactions between protons, and between protons and other nuclei, usually determine[25] the NMR linewidth. The second moment of the low-temperature proton line shape can be quite sensitive to changes in the distribution of hydrogen in this rigid lattice, and it can provide useful information on the site occupancy of hydrogen especially when neutron diffraction data are not available.[16]

In order to test the hypothesis of the preceding section concerning hydrogen site occupancy in $LaNi_4B$ hydride, M_2 measurements were made on a specimen having the composition $LaNi_4BH_{1.5}$. Rigid-lattice proton line shapes were observed below 180 K for this hydride and the M_2 value determined at 78 K was 4.65 ± 0.26 G^2. A sample of $LaNi_5H_{6.0}$ produced the M_2 value 12.6 ± 0.5 G^2 at 78 K which is in favorable agreement with previously reported values for this hydride.[1,2]

Different models of hydrogen site occupancy in $LaNi_4BH_{1.5}$ can be tested by comparing the experimentally determined second moment with values calculated for certain assumed proton distributions. The rigid-lattice second moment of a powdered metal hydride is given by the relation[25]

$$M_2=\tfrac{3}{5}(\gamma_I\hbar)^2I(I+1)\sum_i r_i^{-6}+\sum_k \tfrac{4}{15}(\gamma_{S_k}\hbar)^2 f_k S_k(S_k+1)\sum_j r_{kj}^{-6}\,. \quad (1)$$

In this expression $I=\frac{1}{2}$ is the nuclear spin of the proton, γ_I is the proton gyromagnetic ratio, k distinguishes the different types of metal atoms, f_k is the natural abundance of metal atoms of type k, S_k is the nuclear spin of metal atoms of type k, γ_S is the gyromagnetic ratio for the metal atom of type k, and $\hbar=h/2\pi$ where h is Planck's constant. The sum $\sum_i r_i^{-6}$ extends from a typical proton site to all other sites occupied by protons, and the sum $\sum_j r_{kj}^{-6}$ extends from the same origin used in the proton sum to all sites occupied by metal atoms of type k. In the case of $LaNi_4BH_{1.5}$ the contributions of ^{61}Ni can be omitted from the calculation due to the low natural abundance and small nuclear moment of this isotope, but the contributions of ^{139}La and the two boron isotopes, ^{10}B and ^{11}B, cannot be ignored. The structural model of the hydride must therefore describe the spatial relationships between protons and these other nuclei, in addition to describing the proton sublattice. We will use the $CeCo_4B$ structure as a starting point for the analysis that follows, and we assume that the $P6/mmm$ space group is retained by $LaNi_4BH_{1.5}$.

The most probable locations for hydrogen in $LaNi_4BH_{1.5}$ can be deduced from existing models for deuterium site occupancy in $LaNi_5D_6$ because of the close relationship between the structures of $LaNi_5$ and $LaNi_4B$. A consensus regarding the space group of $LaNi_5D_6$ has not been reached, however, and both the $P31m$ (Refs. 7–9) and $P6/mmm$ (Ref. 6) space groups have been proposed. For our purposes the major differences between the two are the number and type of sites occupied by deuterium. In the $P31m$ space group, deuterium is situated in two types of sites ($3c$ and $6d$) whereas in the $P6/mmm$ space group five different types of sites contain deuterium ($3f$, $4h$, $6m$, $12n$, and $12o$). Since the $3c$ and $6d$ sites in the $P31m$ structure are analogous to the $3f$ and $6m$ sites in the $P6/mmm$ structure, respectively, we will use the site designations of the $P6/mmm$ space group in order to simplify the following discussion. However, because of the doubled $CaCu_5$ arrangement in the $CeCo_4B$ structure, the point symmetry of the $6m$ sites has changed and their Wyckoff notation becomes $12o$. Two types of $12o$ sites must therefore be considered. Sites of the first type, designated $12o^{\mathrm{I}}$ [typical coordinates $(x,2x,0.287)$], are derived from the $6m$ sites of the $LaNi_5D_6$ structure. Sites of the second type are labeled $12o^{\mathrm{II}}$ [approximate coordinates $(x,2x,0.17)$] and are derived from the $12o$ sites of the $P6/mmm$ model for $LaNi_5D_6$. The point symmetries of the $3f$ sites [located at $(\frac{1}{2},0,0;0,\frac{1}{2},0;\frac{1}{2},\frac{1}{2},0)$] and the $12n$ sites [with typical coordinates (0.46,0,0.06) estimated from the positions of the $12n$ sites in $LaNi_5D_6$] have not changed and retain their designations. The locations of these sites in the $CeCo_4B$ unit cell are indicated in Fig. 4.

Considering the small hydrogen capacity of $LaNi_4BH_{1.5}$ and recognizing the high affinity lanthanum has for hydrogen, it is reasonable to assume that hydrogen is situated in those sites closest to the rare-earth positions. The most likely models for hydrogen site occupancy in this hydride therefore involve the $3f$ and $12n$ locations which form a cluster of sites between the lanthanum atoms in the La-Ni basal plane. The minimum allowable H-H separation in intermetallic hydrides is generally recognized[26] as being 2.1 Å, but the maximum separation between sites within the $3f$-$12n$ cluster is about 0.9 Å. It follows that only one hydrogen atom can be accommodated in each cluster. There are two $LaNi_4B$ formula units in each $CeCo_4B$-type unit cell, so the stoichiometry of the true $LaNi_4BH_{1.5}$ unit cell is given by $La_2Ni_8B_2H_3$. This hydrogen composition can be achieved by complete filling of the $3f$-$12n$ clusters. Another alternative would be to fill the $3g$ sites $[(\frac{1}{2},0,\frac{1}{2};0,\frac{1}{2},\frac{1}{2};\frac{1}{2},\frac{1}{2},\frac{1}{2})]$ located between the lanthanum atoms in the La-B midplane. The $3g$ sites are not shown in Fig. 4, but they are analogous to the $3f$ sites in the La-Ni basal plane. Since the c_0/a_0 ratio tends to decrease in $LaNi_4BH_z$ as the volume increases with z,

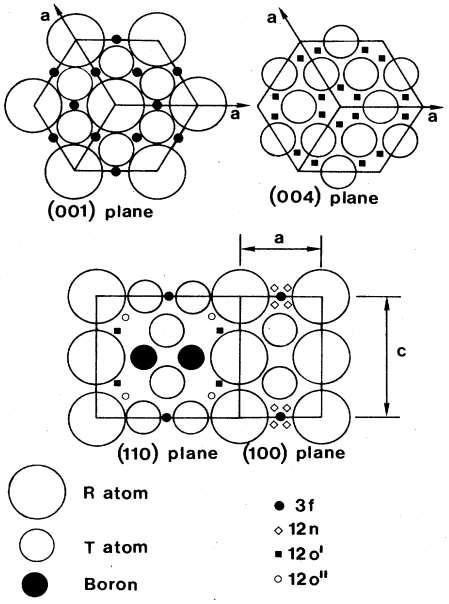

FIG. 4. Sections of the $CeCo_4B$ structure showing locations of sites possibly occupied by hydrogen. Site labels assume the $P6/mmm$ space group. Note that the $6i$ transition-metal layer labeled (004) is located at $z=0.287$. The $3g$ sites (not shown) are analogous to the $3f$ sites except they are located within the R-B midplane ($z=\frac{1}{2}$).

the change in lattice parameters with hydrogen capacity in $LaNi_4B$ hydride do not support the idea that the $12o^{I}$ and $12o^{II}$ sites contain a substantial amount of hydrogen; hence, occupation of these sites was not considered.

Theoretical M_2 values were calculated by assuming that hydrogen was situated in the $3f$-$12n$ clusters in either of two manners; total occupation of only the $3f$ sites, or exclusive occupation of the $12n$ sites with the restriction that only one proton could occupy the four n sites clustered about each vacant f site. Although the protons could be randomly distributed among the sites in the $12n$ clusters, it is believed that an arrangement with maximum average H-H separations would be preferred. A computer program was therefore written to search for the configuration with the maximum average H-H separation within a single La-Ni plane. Starting from a random initial proton occupancy on the $12n$ sites (but, with only one proton per four-site cluster), the computer redistributed the proton occupancies on the $12n$ sites until a maximum average H-H separation distance was found. Convergence was relatively rapid and an examination of proton positions for this configuration indicated an ordered structure. The ordered proton arrangement on the $12n$ sites is easily envisioned as hydrogen atoms equally spaced in rows parallel to the a_0 axis, with adjacent rows lying on opposite sides of the La-Ni plane. This procedure was repeated for several different initial random occupancies on the $12n$ sites and always yielded the same ordered arrangement for the protons. M_2 calculations were also performed for a model in which only the $3g$ sites were completely filled. The results of the calculations described above are summarized in Table II. For comparative purposes we also

TABLE II. Calculated dipolar rigid-lattice second moments (M_2) for $LaNi_4BH_{1.5}$ with the $CeCo_4B$ structure. The total moment M_2 is given by the sum $M_{HH}+M_{HLa}+M_{HB}$ for the partial contributions from dipolar interactions of protons with protons, ^{139}La, and the B isotopes, respectively. All quantities are in units of G^2.

Hydrogen Site Occupancy	M_{HH}	M_{HLa}	M_{HB}[a]	Total[b] M_2
$3f$	4.85	0.48	0.13	5.46
$3g$	4.85	0.48	12.13	17.47
$12n$ (ordered)	3.98	0.51	0.15	4.64

[a]Calculated assuming normal abundance of ^{10}B and ^{11}B isotopes in a random occupancy of the boron sites.
[b]The calculated M_2 values should be compared to the experimentally observed moment 4.65 ± 0.25 G^2.

performed similar calculations for different metal atom structures having antiphase domains, but the results were not significantly different from those obtained with the $CeCo_4B$-type subcell. This is not surprising because it reflects the dominance of the subcell structure in the long-period superlattice models.

The calculated dipolar M_2 values in Table II show that the ordered arrangement of hydrogen on the $12n$ sites gives the best agreement with the observed value 4.65 G^2. Exclusive occupation of the $3f$ sites results in a calculated M_2 value that is somewhat higher than the experimental value, indicating that the protons are positioned too close to each other in this model. Moreover, it is quite clear from the results for the $3g$ site-occupancy model that hydrogen does not occupy sites in the vicinity of the La-B plane. Plausible reasons for this are suggested by looking more closely at the $CeCo_4B$ structure. The nearest-neighbor B-B distance in this structure is 3.1 Å, indicating that interactions between boron atoms are minimal (a separation of about 1.7 Å appears necessary for boron pair formation[27]. However, the displacement of the $6i$ nickel layers towards the La-B midplane results in a nickel-boron separation of 2.1 Å which is somewhat less than the sum of the atomic radii; this implies a strong nickel-boron interaction which apparently acts to exclude hydrogen from the region of the La-B plane. Such reasoning also supports the idea that hydrogen should be excluded from sites within the $6i$ nickel layers. In the case of the long-period superstructure, it is reasonable to assume that nickel-boron interactions are also present near the antiphase boundaries so that hydrogen should be excluded from these regions as well.

The finding that sites near the La-B plane are unfavorable for hydrogen occupancy indicates that these planes may act as barriers to hydrogen motion along the [001] direction. This is significant because long-range diffusion should therefore involve jumps between sites within the La-Ni basal planes. This topic is considered in more detail in the following section.

E. T_1 and $T_{1\rho}$ measurements: hydrogen diffusion

Measurements of the proton relaxation times T_1 and $T_{1\rho}$ by NMR methods have proven to be very useful for

probing the diffusion behavior of hydrogen in metal hydrides.[3–5,25] As a proton moves through a metal hydride it experiences randomly varying dipolar fields. When proton-proton dipolar interactions are the only factors contributing to proton relaxation, the measured proton relaxation times T_1 and $T_{1\rho}$ are given by the relations[25]

$$T_1^{-1}=\tfrac{3}{2}\gamma_I^4\hbar^2 I(I+1)[J^{(1)}(\omega_0)+J^{(2)}(2\omega_0)] , \quad (2)$$

$$T_{1\rho}^{-1}=\tfrac{3}{8}\gamma_I^4\hbar^2 I(I+1)[J^{(0)}(2\omega_1)+10J^{(1)}(\omega_0)+J^{(2)}(2\omega_0)] . \quad (3)$$

In these expressions, $\omega_0=\gamma_I H_0$ is the Larmor frequency where H_0 is the applied field, and $\omega_1=\gamma_I H_1$ where H_1 is the spin-locking field. $J^{(q)}(\omega)$ is the spectral density function of the varying dipolar interactions and is given by

$$J^{(q)}(\omega)=\int_{-\infty}^{\infty} G^{(q)}(t)e^{-i\omega t}dt , \quad (4)$$

where $G^{(q)}(t)$ is the correlation function describing the time dependence of the dipolar interactions. According to a model proposed by Bloembergen *et al.*,[28] known as the Bloembergen-Purcell-Pound (BPP) model, the dipolar interactions decay exponentially with a characteristic time τ_c called the correlation time. With this model, Eq. (4) takes the form

$$J^{(q)}(\omega)=G^{(q)}(0)\frac{2\tau_c}{1+\omega^2\tau_c^2} . \quad (5)$$

Because τ_c is usually equated with the time between jumps,[29] the BPP model provides a link between the proton hopping frequency τ_c^{-1} and the proton relaxation times. Although the absolute values for the proton hopping frequencies obtained from the BPP model may be in error by as much as 50%, the activation energies obtained from the exponential temperature dependence of τ_c^{-1} are found to be within 10% of values obtained by other methods.[25] As a comparative tool, therefore, BPP theory normally provides trends in E_a that are sufficient to characterize the relative differences in the hydrogen diffusion behavior in different metal hydrides.

Possible contributions from heteronuclear dipolar interactions[29] are not included in Eqs. (2) and (3). This approximation is justified for the hydride $LaNi_4BH_{1.5}$ since the H-H dipolar interactions are much greater than the H-La and H-B terms. As shown in Table II, more than 85% of the theoretical M_2 value for $LaNi_4BH_{1.5}$ arises from H-H term in both the $12n$ and $3f$ hydrogen site occupancy models. Since the heteronuclear H-La and H-B terms give only minor contributions to the proton second moment for $LaNi_4BH_{1.5}$, these interactions will also have relatively small effects on the proton relaxation rates[25,29,30] that are induced by diffusion. Because the hydrogen content is 4 times greater for $LaNi_5H_6$, the H-H contributions to M_2 and the dipolar relaxation times are proportionally larger, which further reduces the influence of the H-La contribution in this hydride. Consequently, we do not expect the heteronuclear terms to have any significant roles (i.e., less than 20%) in the total dipolar relaxation rates for both $LaNi_5H_6$ and $LaNi_4BH_{1.4}$, nor to influence the activation energies derived from the proton relaxation times.

The temperature dependences of the measured proton relaxation times T_1 and $T_{1\rho}$ are given in Fig. 5 for specimens having the compositions $LaNi_4BH_{1.4}$ and $LaNi_5H_{6.0}$. An upper temperature limit of about 310 K was chosen for the latter hydride in order to avoid exposing the sealed NMR tube to large internal pressures caused by sample desorption. Inspection of the $LaNi_4BH_z$ pressure-composition isotherms indicated that 333 K should be an upper temperature limit for the $LaNi_4BH_{1.4}$ sample if significant hydrogen losses from the hydride were to be prevented. Exponential recoveries were generally observed for both T_1 and $T_{1\rho}$, except for $T_{1\rho}$ measurements of $LaNi_5H_{6.0}$ in the approximate temperature range 140—190 K. Nonexponential behavior was observed in this region and two $T_{1\rho}$ values could be separated, as indicated in Fig. 5. In this same temperature region the proton line shapes obtained from the $LaNi_5H_{6.0}$ sample exhibited both rigid-lattice and partially narrowed components, with the narrowed component disappearing below about 150 K. Below 140 K the $T_{1\rho}$ recoveries for $LaNi_{5.0}H_{6.0}$ were once again exponential within experimental accuracy. Rigid-lattice line shapes were obtained below 180 K for $LaNi_4BH_{1.4}$. The $T_{1\rho}$ recoveries for $LaNi_4BH_{1.4}$ were always exponential within experimental accuracy.

The minima in the curves shown in Fig. 5 indicate that diffusion is the dominant relaxation mechanism, but diffusion is only one factor that influences the measured values of T_1 and $T_{1\rho}$ in metal hydrides. Interactions with conduction electrons and localized paramagnetic impurities also provide mechanisms for proton relaxation and contribute to the overall spin-lattice relaxation rate according to the relation[30]

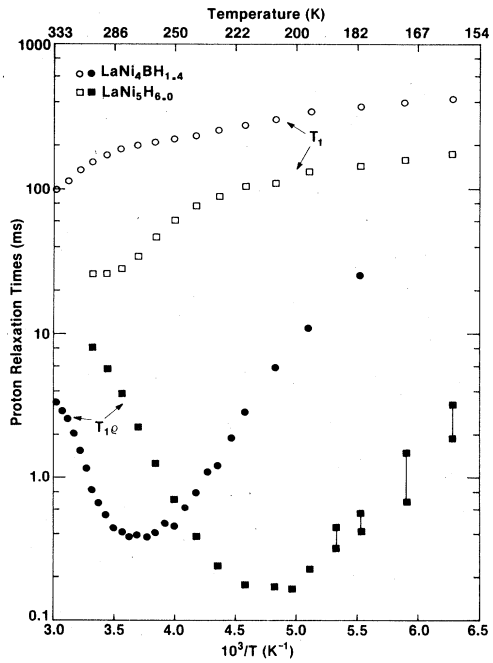

FIG. 5. Temperature dependences of the proton T_1 and $T_{1\rho}$ data for $LaNi_5H_{6.0}$ and $LaNi_4BH_{1.4}$. The vertical lines connect regions of nonexponential recovery.

$$(T_1)^{-1}=(T_{1d})^{-1}+(T_{1e})^{-1}+(T_{1p})^{-1}\,, \tag{6}$$

where T_{1d} represents relaxation processes due to diffusion, T_{1e} represents processes due to interactions with conduction electrons, and T_{1p} arises from processes due to interactions with paramagnetic impurities. A similar relation for $T_{1\rho}$ can also be written.

Contributions from paramagnetic impurities should be minimal when using high-purity starting materials as employed in this study. However, Phua *et al.*[31] have recently found that very small quantities of paramagnetic impurities (e.g., Gd concentrations $\gtrsim 10$ ppm) will significantly contribute to proton relaxation in various binary hydrides. Paramagnetic effects were particularly large for T_1 relaxation in those temperature regions where proton diffusion was expected to be the dominant relaxation mechanism. Consequently, Phua *et al.*[31] warned against assigning any anomalous T_1 behavior as due exclusively to the diffusion processes until the T_{1p} relaxation term has been identified. Figure 6 shows the proton T_1^{-1} behavior at low temperatures for the $LaNi_5H_{6.0}$ and $LaNi_4BH_{1.4}$ samples employed in this study. Since T_1^{-1} for these samples extrapolate to about 0 s^{-1} at 0 K, any paramagnetic effects to their proton relaxation times must be very small[31] and will therefore be ignored. T_{1e} can be evaluated from the low-temperature T_1 data in Fig. 6, where T_{1e} is the dominant term by using the Korringa relation[30]

$$T_{1e}T=C_K\,. \tag{7}$$

In this expression T is absolute temperature and C_K is a constant. The diffusion relaxation times T_{1d} and $(T_{1\rho})_d$ were evaluated at different temperatures by using the experimentally determined values $C_K=66.4$ s K for $LaNi_4BH_{1.4}$ and $C_K=27.2$ s K for $LaNi_5H_{6.0}$, and by assuming $(T_{1\rho})_e=T_{1e}$.

As described in Ref. 5, it is also possible to use the expression

$$(T_{1\rho})_c^{-1}=T_{1\rho}^{-1}-T_1^{-1} \tag{8}$$

to analyze the proton $T_{1\rho}$ data. This procedure not only corrects for the $(T_{1\rho})_e$ contribution, but it also approximately eliminates the $J^{(1)}(\omega_0)$ and $J^{(2)}(2\omega_0)$ terms. Equations (3) and (5) indicate that $(T_{1\rho})_c^{-1}$ should be dominated by the term $\tau_c/(1+4\omega_1^2\tau_c^2)$. Therefore, $(T_{1\rho})_c$ will be inversely proportional to τ_c for $4\omega_1^2\tau_c^2\ll 1$ (i.e., temperatures above the $T_{1\rho}$ minimum) and directly proportional to τ_c for $4\omega_1^2\tau_c^2\gg 1$ (i.e., temperatures below the minimum). If a single jump process describes the diffusion process, τ_c obeys an Arrhenius relation[28–30]

$$\tau_c^{-1}=\tau_0^{-1}\exp(-E_a/k_BT)\,, \tag{9}$$

where τ_0^{-1} is the attempt frequency, E_a is the activation energy, and k_B is the Boltzmann's constant. In this case, the slopes of $\ln(T_{1\rho})_c$ versus T^{-1} plots should yield equal E_a values on both sides of the $(T_{1\rho})_c$ minimum.

The temperature dependences of T_{1d} and $(T_{1\rho})_c$ for $LaNi_5H_{6.0}$ and $LaNi_4BH_{1.4}$ are presented in Fig. 7. The $(T_{1\rho})_c$ slopes above and below the minima are clearly not equal for both samples, which suggest that more than one diffusion process is occurring in these hydrides. Similar behavior should also be observed in the T_{1d} plots, but the T_{1d} minima could not be established because hydride desorption prevented measurements at higher temperatures. The E_a values from Fig. 7 are summarized in Table III along with previously reported results[5] for high-purity $LaNi_5H_{6.2}$ and $LaNi_4AlH_{4.3}$.

The temperature dependences of the proton jump frequency τ_c^{-1} can be obtained from the $(T_{1\rho})_d$ data by solving the expression (also based on the BPP model) given by Korn and Goren,[32]

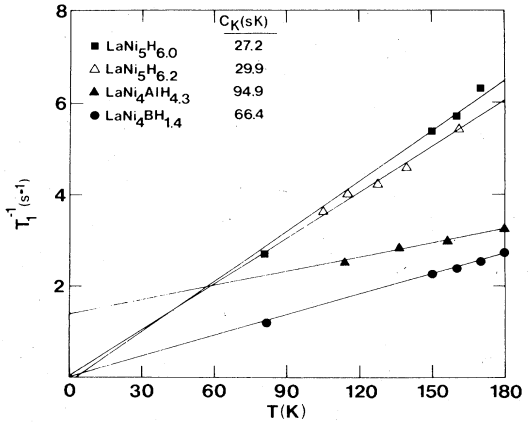

FIG. 6. Temperature dependence of the measured proton T_1^{-1} values in high-purity $LaNi_5H_{6.0}$ and $LaNi_4BH_{1.4}$ at low temperatures. The data for the $LaNi_5H_{6.2}$ and $LaNi_4AlH_{4.3}$ samples are from Ref. 5. The solid lines are extrapolated to the absolute temperature from the lower-temperature data points. The resulting Korringa constants (C_K) are also shown.

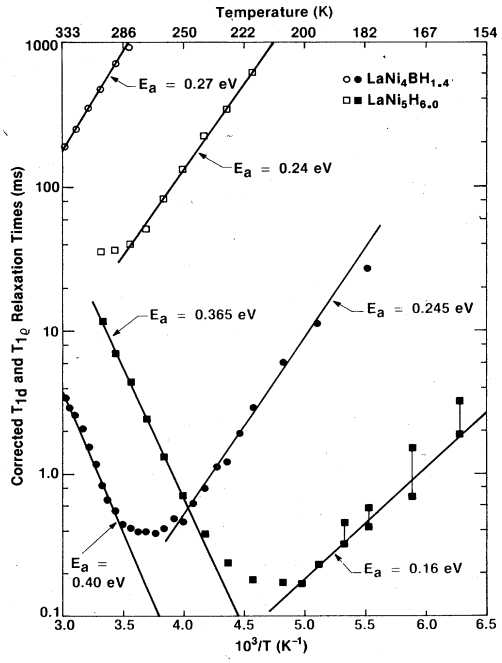

FIG. 7. Temperature dependences of T_{1d} and $(T_{1\rho})_c$ for $LaNi_5H_{6.0}$ and $LaNi_4BH_{1.4}$. The vertical lines connect regions of nonexponential recovery.

$$(T_{1\rho})_d^{-1} = \tfrac{4}{3}(T_{1\rho})_{d,\min}^{-1}\left[\frac{3y}{y^2+4}+\frac{5y}{y^2+a^2}+\frac{2y}{y^2+4a^2}\right]. \quad (10)$$

Here, $(T_{1\rho})_{d,\min}$ is the minimum value of $(T_{1\rho})_d$, $y=(\tau_c\omega_1)^{-1}$, and $a=\omega_0/\omega_1$. The values of τ_c^{-1} obtained from this equation are plotted versus T^{-1} in Fig. 8, where we have also included the results obtained from analysis of the previously measured[5] $T_{1\rho}$ data for the $LaNi_5H_{6.2}$ and $LaNi_4AlH_{4.3}$ samples. In addition to showing that the proton mobilities in $LaNi_4BH_{1.4}$ and $LaNi_4AlH_{4.3}$ are substantially reduced from that found in $LaNi_5H_6$, the curves in this figure also reveal more than one E_a value for each hydride. The arrows indicate the temperature of the $(T_{1\rho})_d$ minima and show that they are different from the temperatures at which the slopes abruptly change. Equation (10) was not used to estimate τ_c^{-1} in regions of nonexponential $T_{1\rho}$ recoveries for the two $LaNi_5H_6$ samples (i.e., below the $T_{1\rho}$ minima) because assignment of proper ratios becomes very ambiguous. Since the $T_{1\rho}$ recoveries for $LaNi_4BH_{1.4}$ and $LaNi_4AlH_{4.3}$ were exponential throughout their measured ranges, it was possible to use Eq. (10) below the $(T_{1/\rho})_d$ minimum for these latter samples. A summary of the E_a values from Fig. 8 is included in Table III where the temperature ranges used to derive each activation energy are also given. In later discussions, the terms "high temperature" and "low temperature" will denote parameters that correspond to temperatures above and below, respectively, the individual minima for both the T_1 and $T_{1\rho}$ relaxation times.

Before discussing the E_a parameters and possible diffusion mechanisms in more detail, some possible effects due to the magnetic nickel species[12–14] need to be addressed. Previous NMR studies[3–5] of $LaNi_5H_6$ have

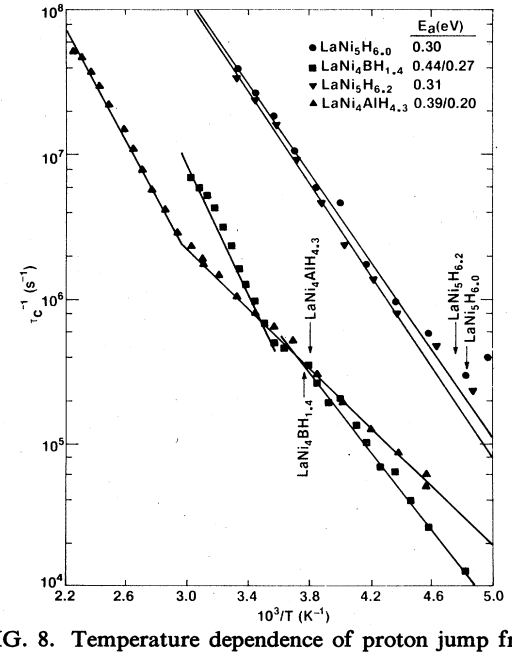

FIG. 8. Temperature dependence of proton jump frequency (τ_c^{-1}) in $LaNi_5H_6$, $LaNi_4AlH_{4.3}$, and $LaNi_4BH_{1.4}$. Arrows indicate temperatures of the $(T_{1\rho})_d$ minima for each sample.

TABLE III. Summary of E_a values obtained from Figs. 7 and 8. The temperature ranges for which each E_a was obtained are also listed. See the text for discussions of temperature differences in E_a values.

Source	$LaNi_5H_{6.0}$ Temperature Range (K)	E_a (eV)	$LaNi_5H_{6.2}$[a] Temperature Range (K)	E_a (eV)	$LaNi_4AlH_{4.3}$[a] Temperature Range (K)	E_a (eV)	$LaNi_4BH_{1.4}$ Temperature Range (K)	E_a (eV)
T_{1d} (Fig. 7)[b]	222–310	0.24(1)	208–291	0.22(2)	239–387	0.16(2)	280–333	0.27(1)
$(T_{1\rho})_c$ (Fig. 7)[c]	250–310	0.37(1)	229–301	0.37(1)	322–445	0.44(1)	286–333	0.40(1)
	160–200	0.16(2)	146–194	0.16(1)	197–260	0.13(1)	200–250	0.25(2)
$(T_{1\rho})_d$ (Fig. 8)[d]	204–294	0.30(2)	204–294	0.31(1)	357–435	0.39(1)	294–333	0.44(2)
					217–333	0.20(1)	208–278	0.27(2)

[a]Data from Ref. 5.
[b]Data only available for temperatures below T_{1d} minimum.
[c]E_a values from $(T_{1\rho})_c$ data based upon approximation which includes only the first term in Eq. (3).
[d]$(T_{1\rho})_d$ data for the $LaNi_5H_6$ samples were not analyzed with Eq. (10) in regions of nonexponential recoveries.

clearly shown that large quantities (i.e., $\gtrsim 0.1$ at. %) of paramagnetic impurities (i.e., other rare-earth metals, Fe, or Mn) and/or precipitated nickel can profoundly influence proton relaxation times as well as the derived diffusion parameters. Reliable NMR studies of proton diffusion behavior therefore require that only metals with minimal amounts of potential paramagnetic impurities be used to prepare the hydride samples. The recent observations of Phua, *et al.*[31] dramatically reinforce this criterion. The four $LaNi_{5-x}M_xH_z$ samples whose E_a values are given in Table III are believed to satisfy this requirement with regard to chemical impurities. However, the magnetic behavior of the $LaNi_5$ and $LaNi_4B$ powders that was described in Sec. II B implies small (but finite) quantities of superparamagnetic nickel also exist in the corresponding NMR samples even though the bulk intermetallics were crushed under helium before preparing the hydrides. Karlicek[3] has described in his thesis how the proton $T_{1\rho}$ values and line shapes can be influenced by the presence of free nickel, which is presumably located on the surfaces of the hydrides particles.[12,3] Excessive nickel gave shifted and anomalously broad $T_{1\rho}$ minima as well as reduced spin-echo linewidths.[3] Within the extent that the data can be directly compared, the present $LaNi_5H_{6.0}$ and $LaNi_4BH_{1.4}$ samples correspond to the best samples (i.e., least amounts of free nickel and other magnetic impurities) of both Karlicek and Lowe[3] and Bowman *et al.*[4,5] Furthermore, the low-temperature T_1 data in Fig. 6 for the two $LaNi_5H_6$ samples and $LaNi_4BH_{1.4}$ are entirely consistent with relaxation by the Korringa process.[30] Hence, any paramagnetic relaxation effects from the precipitated nickel at the surfaces that would correspond to phenomena described by Phua *et al.*[31] seem very unlikely for these samples. Although Fig. 6 indicates that some form of paramagnetic relaxation occurs for the $LaNi_4AlH_{4.3}$ sample, there do not appear to be any large effects for the other relaxation times.[5] Because it appears to be extremely difficult[3–5] to prepare powdered NMR samples of $LaNi_{5-x}M_xH_z$ materials that completely avoid the creation of free nickel, diffusion studies will probably be limited to samples prepared from high-purity metals but containing some minimal quantities of magnetic nickel. We believe that the samples listed in Table III should be of adequate chemical and magnetic purities for reliable evaluations of their diffusion properties.

The observations of multiple E_a values for $LaNi_4BH_{1.4}$ and $LaNi_5H_{6.0}$ are consistent with the results of other studies which indicate complex diffusion behavior in $LaNi_5H_6$ (Refs. 3 and 5) and $LaNi_{5-x}Al_xH_z$ ($0 \leq x \leq 1.5$) (Ref. 5). In the latter hydrides it was found that the diffusion coefficient decreased by more than 2 orders of magnitude as aluminum content increased,[4] primarily because the E_a value for the high-temperature process increased with x for $x > 0.5$ (aluminum substitution had little influence on the E_a value of the low-temperature process, however[5]). This observation led to the suggestion that the large aluminum atoms in $LaNi_{5-x}Al_x$ hydrides may restrict the low-energy diffusion pathways.[5] However, neutron diffraction experiments on $LaNi_{4.5}Al_{0.5}D_{4.5}$ (Ref. 33) and $LaNi_4AlD_{4.8}$ (Ref. 6) reveal that, although the $12o$ and $4h$ sites were empty, a substantial amount of deuterium is located in the $6m$ sites within the $3g$ metal layers which contain aluminum (when the $P6/mmm$ space group[33] is retained by the deuterides). Even with the assignment of the $P321$ space group for the $LaNi_{5-x}Al_xD_z$ structures, Yartys *et al.*[34] found that a significant amount of deuterium remained in the midplane region near the Al atoms, although there was a large reduction in the deuterium site occupancy of the $6g_1$ sites (nearly equivalent to the $6m$ sites in the $P6/mmm$ space group) in $LaNi_4AlD_{4.1}$ when compared to $LaNi_5D_{6.0}$. Hydrogen motion along the [001] direction and through the metal layers containing aluminum therefore appears quite likely, and the aluminum atoms themselves do not seem to be the direct cause of the increased E_a values. In contrast, hydrogen motion in $LaNi_4BH_{1.4}$ should be severely restricted in directions perpendicular to the La-B midplane since hydrogen does not occupy sites in the vicinity of this layer. Despite these differences, both $LaNi_4AlH_{4.3}$ and $LaNi_4BH_{1.4}$ exhibit E_a values of similar magnitude and which are large relative to that observed in $LaNi_5H_6$. This suggests that the trend towards larger E_a values in the substituted hydrides must be caused by factors other than a straightforward blockage of jump paths.

In order to assess the hydrogen diffusion processes in these $LaNi_{5-x}M_x$ hydrides we wish to more closely examine the E_a values in Table III that were derived from the $(T_{1\rho})_c$ data for temperatures above the minima. Since the procedure used to obtain $(T_{1\rho})_c$ has greatly reduced the $J^{(1)}(\omega_0)$ and $J^{(2)}(2\omega_0)$ contributions for this temperature range, the E_a values derived from these $(T_{1\rho})_c$ data should directly reflect the long-range diffusion behavior from only the low-frequency contributions to $J^{(0)}(2\omega_1)$. By using a special version of the pulsed field gradient NMR technique, Karlicek and Lowe[3] measured the hydrogen diffusion constants in β-$LaNi_5H_{6.5}$ and obtained an activation energy of 0.42(4) eV in the temperature range 330—375 K. Within the combined limits of errors, this result agrees with all of the E_a values in Table III that were obtained from the high-temperature $(T_{1\rho})_c$ data. However, the results of the present study indicate that the E_a values for $LaNi_4AlH_{4.3}$ and $LaNi_4BH_{1.4}$ are significantly larger than those for the two $LaNi_5H_6$ samples.

These findings can be rationalized by considering the site occupancy of hydrogen in $LaNi_4BH_{1.4}$, $LaNi_4AlH_{4.3}$, and $LaNi_5H_6$. The neutron diffraction studies[6] which use the $P6/mmm$ space group for $LaNi_4AlD_{4.8}$ indicate that the $12o$ sites in this deuteride are completely empty; only the $12n$ and $6m$ sites contain deuterium. By the arguments of the preceding section, analogous sites in $LaNi_4BH_{1.5}$ ($12o^{II}$ sites in Fig. 4) are also unoccupied at 78 K and are not likely to be substantially occupied at higher temperatures. If we consider the hydrogen jump paths $12n$-$12o$-$6m$ for $LaNi_4AlH_{4.3}$ and $12n$-$12o^{II}$-$12n$ for $LaNi_4BH_{1.4}$, we see that the intermediate step in these jump sequences involves passage through the $12o$ sites which are unfavorable for occupation by hydrogen. (We should also note that the antiphase domain structure of $LaNi_4B$ does not alter the proposed jump sequence in $LaNi_4BH_{1.4}$ because the subcells in each domain retain the $CeCo_4B$ atomic arrangement.) However, the $12o$ sites are occupied to a significant extent in $LaNi_5H_6$ and they

should consequently present lower barriers for both jump mechanisms in this hydride. These diffusion models are consistent with both the "tunnel" model proposed by Halstead,[1] and the proton jump sequence $3f$-$12n$-$12o$-$6m$-$12o$-$12n$ suggested by Achard *et al.*[35] for the $P6/mmm$ space-group model of $LaNi_5H_6$. Schematic representations of possible E_a profiles for the proposed jump sequences are given in Figs. 9(a) and 9(b). Differences in potential well depths between the $12n$ and $6m$ sites are ignored for simplicity in these figures, but a substantial difference between $12o$ well depths in $LaNi_5D_{6.5}$ and $LaNi_4AlD_{4.8}$ has been assumed because of the significant differences between $12o$ site occupancies for these deuterides at room temperature. These E_a profiles are also compatible with the recent proposal by Westlake[36] that interstitial site dimensions preclude $12o$ site occupancy in $LaNi_4AlD_{4.8}$ but not in $LaNi_5D_{6.5}$. Furthermore, a reduced $12o$ interstitial hole radius and a shallow well depth are also suggested for $LaNi_4BH_{1.4}$ because the lattice parameters of this hydride (normalized to the $CaCu_5$ structure) are smaller than those of both of these deuterides. Geometric restrictions and the intermediary role of the $12o$ site are therefore plausible reasons for the absence of any observable hydrogen in the $12o$ sites of the substituted hydrides.

An alternative viewpoint for understanding the diffusion behavior in $LaNi_{5-x}M_x$ hydrides comes from considering the influence of substitution on the heights of the saddle points separating the potential wells of adjacent sites. Westlake[36] used the radii of the largest holes in trigonal faces that hydrogen must pass through as a measure of saddle-point height, and presented data for various saddle points in $LaNi_5D_{6.5}$. In Table IV we summarize the results of similar calculations for the $12o$-$6m$ and $12o$-$12n$ saddle points in $LaNi_4AlD_{4.8}$ and $LaNi_4BH_{1.5}$. The radii in this table indicate a tighter fit through the trigonal faces in the substituted hydrides when compared to similar jumps in $LaNi_5D_{6.5}$, and they are in agreement with the trend in E_a values shown in Table III. The E_a profile for a diffusion process limited by saddle-point barriers is illustrated in Fig. 9(c). Hence, we see that Westlake's recent suggestion[36] that the $12o$ sites are crucial to long-range diffusion is supported by considering either a reduced $12o$ well depth or an increased saddle-point height in substituted hydrides. Of course, it is possible that both factors may be simultaneously influencing the diffusion process.

TABLE IV. Radii of largest holes in trigonal faces joining interstitial sites (in Å).

Site pair	$LaNi_5D_{6.5}$[a]	$LaNi_4AlD_{4.8}$[a]	$LaNi_4BH_{1.4}$
$12o$-$6m$	0.383	0.355[b]	0.316
		0.295[c]	
$12o$-$12n$	0.316	0.290[b]	0.248
		0.222[c]	

[a]Lattice parameters for the deuterides were taken from Ref. 36. [b]Radii of holes surrounded only by Ni atoms. [c]Radii of holes surrounded only by Ni and Al atoms.

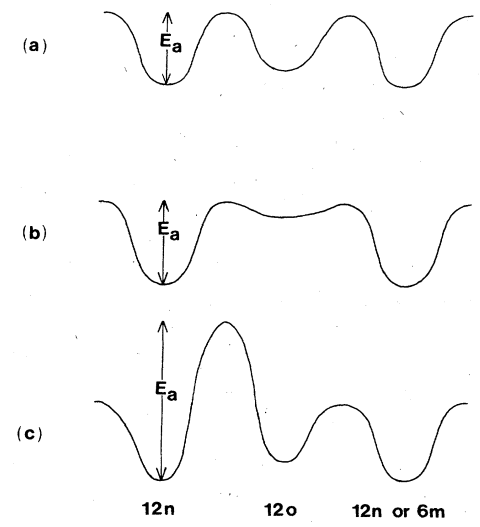

FIG. 9. Schematic E_a profiles for proposed hydrogen jump processes. (a) Intermediate site in $LaNi_5H_6$; (b) intermediate site in $LaNi_4BH_{1.5}$ and $LaNi_4AlH_{4.3}$; (c) saddle-point barrier. The magnitude of E_a in (c) is exaggerated relative to the profiles shown in (a) and (b) in order to more clearly illustrate the difference between the $12n$-$12o$ and $12o$-$6m$ saddle-point heights (see Table IV).

The jump processes which involve the $12o$ sites clearly correspond to long-range hydrogen diffusion mechanisms in $LaNi_5$-type hydrides, but the small E_a processes observed for the low-temperature proton relaxation times appear (i.e., from data for temperatures below the T_1 and $T_{1\rho}$ minima) to be related to a local motion that does not contribute to hydrogen transport.[3,5] Some very recent quasielastic neutron scattering (QNS) experiments[35,37–39] have provided independent evidence for local hopping modes in $LaNi_5H_6$ but, just as there has been no resolution of the β-phase $LaNi_5H_6$ space-group dilemma,[6–8,34] each of the QNS experimental groups has given a different interpretation for the local hydrogen motion. Achard *et al.*[35,37] use the $P6/mmm$ space group and propose that hydrogen hops back and forth among the sites in the $3f$-$12n$ clusters of $LaNi_5H_{5.8}$ and $LaNi_4MnH_{5.7}$ but claim there is no local hopping in $LaNi_4AlH_{4.3}$. Richter *et al.*[38] have suggested that local hopping occurs about unspecified structural traps such as those produced by variations from exact metal stoichiometry. Finally, Noréus *et al.*[39] proposed hopping within the "$6d$ rings" of the $P31m$ space group (the $6d$ sites are very close to the location of the $6m$ sites of $P6/mmm$ but are slightly displaced along the z direction). Since there has been mutual criticism among the QNS papers[38,39] with respect to spectral resolution and data-analysis procedures, it is not easy to assess which QNS experiments (if any) are most reliable. Furthermore, the hydrogen diffusion contributions to the QNS line shapes in $LaNi_5H_6$ samples are quite small (because of relatively slow diffusion rates) and apparently are very difficult to identify. The only agreement among the QNS studies[35,37–39] of $LaNi_5H_6$ is that the diffusion is complex and involves local hopping as well as long-range diffusion.

The preceding discussion has emphasized the $P6/mmm$ structure[6] for the $LaNi_5$-type hydrides over the $P31m$ structure.[7–9] This is partially due to convenience in identifying the jump sites where the $12o$ sites appear to play a dominate role in long-range diffusion. However, within the $P31m$ space group it is also possible to consider unoccupied sites which have an intermediary role linking the occupied $3c$ and $6d$ sites, just as the $12o$ sites were intermediates between the $12n$ and $6m$ sites in the $P6/mmm$ space group. These unoccupied sites would carry the $6d$ Wyckoff label, but would have coordinates which are different from occupied $6d$ sites. Therefore, using the two-site $P31m$ model, it is clear that the saddle-point mechanism must be operative. Otherwise, it would be difficult to envision why the E_a values of the substituted hydrides should be increased relative to those of $LaNi_5H_6$ because the "intermediate-site" description of the jump paths in $LaNi_4MH_z$ (M = Al, B) remain essentially unaltered from those in $LaNi_5H_6$. But it should be noted that the two-site $P31$ model[7–9] for $LaNi_5H_6$ cannot account for the similarities between local hopping behavior in $LaNi_4AlH_{4.3}$ and $LaNi_4BH_{1.4}$ because it lacks the $3f$-$12n$ site clusters of the $P6/mmm$ space group. According to the present NMR studies, as well as some QNS studies,[35,37] the proton hops between the $3f$-$12n$ sites are probably responsible for the short-range motion.

F. Discussion of non-BPP behavior in $LaNi_{5-x}M_xH_z$

The combination of short-range and long-range contributions to τ_c was originally proposed[3,5] because the proton relaxation times in $LaNi_{5-x}M_xH_z$ do not exhibit traditional BPP behavior,[1–5,40] but these deviations seriously limit any quantitative application of the BPP model. Although the field dependences of T_1 and $T_{1\rho}$ were not explicitly determined for the present $LaNi_5H_{6.0}$ or $LaNi_4BH_{1.4}$ samples, Chang *et al.*[40] observed a field dependence of $\omega_1^{-1.35}$ below the $T_{1\rho}$ minimum for $LaNi_{5.0}H_{7.0}$, whereas simple BPP theory predicts a ω_1^{-2} dependence at these low temperatures. Motional relaxation has exhibited non-BPP behavior in many types of solids that include other hydrides,[31,41,42] PbF_2 doped with alkali halides,[43] two-dimensional (2D) crystals,[44–46] organic molecules undergoing reorientational motions,[47–49] and various types of glasses.[50,51] Numerous alternative descriptions have been proposed that either modify or generalize the original BPP model in order to reproduce the anomalous temperature and/or frequency behavior. In this section we will consider several of these alternatives to the BPP model and will relate them, whenever possible, to the available experimental proton relaxation times for $LaNi_{5-x}M_xH_z$.

The relaxation times for mobile nuclei in 2D solids often show[45,46] an approximate $\omega^{3/2}\tau^{1/2}$ dependence at temperatures below their minima, which is consistent with model calculations[52] for continuum 2D diffusion. However, Sholl[53] has subsequently demonstrated that simple jumps of any finite distance will always generate a $\omega^2\tau_c$ dependence for the low-temperature relaxation rates which is independent of the dimensionality of the lattice. Since hydrogen atoms clearly occupy well separated and distinct sites in the $LaNi_{5-x}M_x$ lattices (even if their identifications and occupancy factors have not been unequivocally established,[6–9,33,34] the continuum, liquidlike motions required[53] for the $\omega^{3/2}\tau_c^{1/2}$ behavior are extremely unlikely for these materials. Furthermore, the relative positions of these hydrogen sites do not form 2D networks for either the $12n$-$12o$-$12n$ or $12n$-$12o$-$6m$ jump paths. Hence, 2D diffusion cannot account for the anomalous proton relaxation times in $LaNi_{5-x}M_xH_z$ even though the low-temperature $LaNi_5H_7$ $T_{1\rho}$ data of Chang *et al.*[40] exhibited an $\omega_1^{-1.35}$ behavior and the apparent E_a values below the T_1 and $T_{1\rho}$ minima are approximately half the high-temperature activation energies as shown in Table III. Both of these properties would be consistent with the predictions of the continuum 2D model,[45,46,52] but the proton jump paths in $LaNi_{5-x}M_xH_z$ involve discrete jumps of finite distances in three dimensions.

The non-BPP temperature and frequency dependences of nuclear relaxation times in highly disordered or amorphous solids have been analyzed with various distribution functions[43,44,50,51] for the nuclear correlation times. This approach assumes a quasicontinuous variation for the individual nuclear jumps that arise from differences in the potential barrier heights, which is probably justified whenever there is extensive disorder in the local environments from either large defect concentrations or lack of structural order. While various distribution functions can fit the anomalous nuclear relaxation behavior for several types of solids[43,44,50] (often with physically reasonable activation energy ranges), details of the physical diffusion processes usually remain obscure. Although the distribution function methods[43,44] do predict higher apparent E_a values for temperatures above the T_1 or $T_{1\rho}$ minima as observed in $LaNi_{5-x}M_xH_z$, the retention of structural order for the metal atoms suggests that extensive variations among the several types of occupied and vacant hydrogen potential wells would be unlikely in the present case. Consequently, we do not believe that fitting some form of distribution function[43,44,50] to the proton relaxation times in Fig. 5 would help clarify the causes for anomalous temperature behavior.

Phenomenological spectral density functions[41,49,54,55] have also been proposed to represent relaxation times that do not follow BPP behavior. The approach generally allows[54,55] the spectral density functions $J(\omega)$ to have variable exponents for the parameters ω and τ_c, but it also assumes (without any physical justification) that the motions responsible for the nuclear relaxation exactly obey the Arrhenius relation. While these methods can be made to precisely reproduce experimental data,[49,54] the resulting activation energies and adjustable fitting parameters may provide little useful insight on the actual diffusion process. When Chang, *et al.*[40] used the empirical procedure of Halstead *et al.*[41,54] to analyze the proton relaxation times for $LaNi_5H_7$, they obtained a reasonable E_a in good agreement with the values from direct measurement of the diffusion coefficient[13] and their BPP-like analysis of the high-temperature $T_{1\rho}$ data. However, Chang *et al.*[40] could not explain the peculiar spectral density function that came from this fitting procedure. We believe that forcing the diffusion correlation time to fol-

low an Arrhenius relationship over the entire temperature is responsible for the unusual spectral density function found by Chang *et al.*[40] Consequently, this particular empirical approach will not be very helpful—unless some independent means can establish that τ_c actually follows an Arrhenius relation over the temperature range of the measured relaxation time data. Since such information is not available for the $LaNi_{5-x}M_xH_z$ samples, the various phenomenological analysis methods[41,49,54,55] will not be considered further.

Molecular reorientation between unequal potential wells will produce unusual nuclear-spin relaxation behavior,[47,56] since the BPP expressions are modified by Boltzmann factors that arise from the relative occupancies of the potential wells at different energies. Among the more important consequences[47,56] of this particular mechanism are greatly reduced relaxation rates (i.e., very shallow T_{1d} and $T_{1\rho}$ minima) and unequal slopes about the T_1 and $T_{1\rho}$ minima with the smaller slope occurring for temperatures above the minima. For a threefold rotational potential Anderson[56] showed qualitatively similar behavior whether one or two wells were more stable, although the largest effects occurred when two wells were lower. Polak and Ailion[47] have generalized the analysis for this latter situation and compared their theoretical expressions to the proton relaxation times for solid *trans,trans*-muconodinitrile with considerable success. Because proton hops among unequal potential wells in the $LaNi_{5-x}M_xH_z$ phases were suggested in the preceding section (i.e., see Fig. 9), some comparisons with the asymmetric rotation-model predictions seem appropriate. First, proton $T_{1\rho}$ relaxation times for all $LaNi_{5-x}M_xH_z$ samples have greater slopes above their minima than are found at temperatures below the minima. This behavior is exactly opposite to the predictions of the asymmetric rotation model.[47] Furthermore, Table V shows that the experimental T_{1d} and $T_{1\rho}$ minima for $LaNi_5H_{6.0}$ and $LaNi_4BH_{1.4}$ are both somewhat smaller than the theoretical BPP-model values calculated from the experimental proton M_2 parameters with the procedures described by Karlicek and Lowe.[3] Again, this is completely opposite to the behavior predicted by the rotational model,[47,55] which is apparently not directly applicable to the motions in $LaNi_{5-x}M_xH_z$. However, the above observations do not exclude the possibility that some alternative formulation of jumps among inequivalent potential wells, which more closely corresponds to the actual processes in $LaNi_{5-x}M_xH_z$, could alter the BPP expressions. Fedders[57] has considered simple hops among inequivalent interstitial sites, but his results are too qualitative to be of any real assistance. Consequently, since we do not currently have an adequate theory to quantitatively assess the effects of unequal potential wells, we will continue to use the general BPP model while remembering its limitations.

Qualitative comparisons of the proton relaxation times for $LaNi_5H_6$, $LaNi_4AlH_{4.3}$, and $LaNi_4BH_{1.4}$ provide evidence (albeit often indirect) for the simultaneous presence of local hopping and long-range diffusion processes. First, smaller E_a values are obtained for T_{1d}, $(T_{1\rho})_c$, and $(T_{1\rho})_d$ parameters below their minima when compared to activation energies determined above the minima. Abragam[58] has pointed out that for temperatures above the minimum relaxation is dominated by motions of distant spins, whose positions change according to the macroscopic diffusion properties. In contrast, fluctuations of dipolar interactions between neighbor spins control the relaxation below this minimum. If the same physical process (e.g., simple hops among equivalent sites) is responsible for both the short- and long-range dipolar fluctuations, the equal slopes of the usual BPP model will result. However, local hopping of a proton within a cluster of sites (e.g., the $12n$-$3f$-$12n$ mechanism) is expected to more greatly influence its neighboring protons than those more distant spins, since the site separations for local hopping are much shorter than the jump lengths associated with long-range diffusion.

Consequently, in the temperature ranges between the T_1 and $T_{1\rho}$ minima the T_{1d} and $(T_{1\rho})_d$ will reflect the local hopping and long-range relaxation processes, respectively, to yield the distinctly different E_a values over common temperatures. It is satisfying that the $(T_{1\rho})_c$ and $(T_{1\rho})_d$ data above their minima do give E_a values similar to that directly measured[3] for the long-range proton diffusion coefficient in $LaNi_5H_z$. The smaller E_a values that are obtained from both the T_1 and $T_{1\rho}$ data below their respective minima are consistent with the local hopping involving smaller potential barriers than long-range diffusion. The $12n$-$3f$-$12n$ model of Achard *et al.*[35,37] would be applicable with the proton site occupancies expected for each $LaNi_{5-x}M_xH_z$ sample. Since the smaller E_a values obey the sequence $E_a(LaNi_4AlH_{4.3}) < E_a(LaNi_5H_6) < E_a(LaNi_4BH_{1.4})$, Al and B substitution apparently alters the local hopping potential barriers in opposite directions. The causes of this difference are not clear, but changes in the relative dimensions of the $12n$ and $3f$ sites may be responsible.

At least two types of short-range processes, each with potentially different rates and activation energies (e.g., jumps within the $6m$ rings and hopping within the $3f$-$12n$ clusters) are possible in $LaNi_5H_6$. The simultaneous pres-

TABLE V. Comparisons of BPP-model predicted and experimentally observed T_{1d} and $T_{1\rho}$ minima for $LaNi_5H_{6.0}$ and $LaNi_4BH_{1.4}$, where $\omega_0/(2\pi)=34.5$ MHz and $H_1=7.3$ G.

	T_{1d} (ms)		$T_{1\rho}$ (ms)	
Sample	Theory	Experiment	Theory	Experiment
$LaNi_5H_{6.0}$	36	30	0.173	0.166
$LaNi_4BH_{1.4}$	98	a	0.470	0.381

[a]Minimum could not be observed because measurements were limited to temperatures below 330 K to avoid decomposition.

ence of these processes may be responsible for nonexponential $T_{1\rho}$ recoveries as well as two component proton line shapes seen[2,3,5,40] between about 140 and 200 K for $LaNi_5H_6$. Since nothing similar has been observed for the substituted hydrides, it may be that only the $12n$-$3f$-$12n$ local process is possible in $LaNi_4BH_{1.4}$, while in $LaNi_4AlH_{4.3}$ the Al neighbors to many $6m$ sites could eliminate rapid jumps within the $6m$ rings but still permit $12n$-$3f$-$12n$ hopping. Although segregated phases with different proton mobilities could also produce the effects seen in $LaNi_5H_6$, there has been no other experimental evidence for mixed phases in $LaNi_5H_x$ at these temperatures or compositions. However, the rather strong dipolar interactions expected between protons in $LaNi_5H_6$ would normally produce a common spin temperature in a time on the order of T_2, which is much shorter than the limiting $T_{1\rho}$ values seen in $LaNi_5H_6$ between 140 and 190 K. Wolf[59] has described how the establishment of a spin temperature can become strongly inhibited when H_1 is greater than the local dipolar field, which is just the situation for the $T_{1\rho}$ measurements in $LaNi_5H_6$. Furthermore, Garroway[60] has demonstrated that the decay of rotating frame magnetization can proceed by spin-spin coupling to the dipolar reservoir, which is independent of the lattice motions, under somewhat similar conditions. Although we are not able to prove that two independent local hopping processes actually caused the nonexponential $T_{1\rho}$ recoveries in $LaNi_5H_6$, we feel it is feasible since only exponential $T_{1\rho}$ recoveries are observed for the substituted hydrides. Furthermore, the $LaNi_5H_6$ samples do give exponential recoveries below 140 K, where either only a single-motion process remains or a common spin temperature is established more rapidly.

In summary, after the consideration of several alternative sources for the anomalous proton relaxation time behavior in $LaNi_{5-x}M_xH_z$, we believe that a mixture of local hopping and long-range diffusion processes are probably responsible. The available QNS results[35,37–39] also support this view. The likely proton jump paths in the $LaNi_{5-x}M_x$ hydrides are probably along the sequence of $3f$-$12n$-$12o$-$6m$-$12o$-$12n$ sites as suggested by Achard *et al.*[35] Although we believe passage through the $12o$ sites is necessary for long-range diffusion, the very short separations[6] between the $12n$-$3f$ and $6m$-$6m$ pairs will allow much more rapid localized proton motions that persist to rather low temperatures. However, these local hopping processes will be superimposed upon the long-range diffusion jumps as the temperature increases. Consequently, both types of processes will contribute to the proton relaxation times. When the temperatures are greater than the values required for either T_{1d} or $(T_{1\rho})_d$ minima, the relaxation times should mainly reflect the long-range processes (with the larger activation energies), while the short-range motions (with the expected smaller E_a values) will dominate the relaxation times for temperatures below the minima. Both processes probably give large contributions to the relaxation times for temperatures in the immediate vicinities of the minima. Unfortunately, the currently available models[25,30,40,53,57] that relate proton relaxation times to microscopic jump processes are inadequate to represent the diffusion behavior in a more quantitative fashion. Furthermore, the hydrogen site occupancy controversies[6–9,33,34] for $LaNi_{5-x}M_xH_z$ must first be resolved over the entire temperature range before more detailed models are attempted. It is hoped that the present experimental results and discussion will stimulate such efforts.

IV. CONCLUSIONS

We have found that the hydrogen absorption properties of $LaNi_4B$ are substantially different from those of $LaNi_5$. Proton rigid-lattice second-moment measurements on $LaNi_4BH_{1.5}$ confirm that the small hydrogen capacity in this hydride results from the exclusion of hydrogen from sites in the vicinity of the La-B midplane and $6i$ nickel layers. These same measurements indicate that hydrogen occupies sites located between the lanthanum atoms in the La-Ni basal plane. Thus, $LaNi_4BH_{1.5}$ presents itself as a useful model for understanding hydrogen diffusion in $LaNi_5H_6$ and related systems because the La-B plane should act as a barrier to hydrogen diffusion along the z direction. We conclude from similarities in the diffusion parameters for hydrogen in $LaNi_4BH_{1.5}$ and $LaNi_4AlH_{4.3}$ that the activated step for the long-range jump process in these hydrides is passage through the $12o$ sites, which are otherwise unoccupied, or passage through the holes in the trigonal faces linking the $12o$ sites to other sites. In either case, it appears that the $12o$ site is important for purposes of macroscopic hydrogen transport. There is also evidence that a local hopping process, which does not lead to long-range diffusion, occurs within clusters of sites located in the La-Ni basal planes. These models for hydrogen motion in $LaNi_5$-type hydrides can be readily explained within the framework of the $P6/mmm$ space-group model $LaNi_5H_5$, but are not entirely consistent with the $P31m$ space group.

Additionally, we have found that $LaNi_4B$ crystallizes with a structure that is more complex than the previously reported $CeCo_4B$-type atomic arrangement. Single-crystal data show that $LaNi_4B$ has an antiphase domain structure with $CeCo_4B$-type subcells, but this superstructure is not expected to make any major contribution to either short-range or long-range hydrogen diffusion processes in $LaNi_4BH_{1.5}$.

ACKNOWLEDGMENTS

We wish to thank F. T. Parker for his many useful suggestions and comments. We also thank E. Bucher and K. Ensslen for the use of the facilities at the University of Konstanz, Konstanz, West Germany, where the high-purity $LaNi_5$ and $LaNi_4B$ samples were prepared and characterized, and W.-K. Rhim for the use of his NMR spectrometer at the Jet Propulsion Laboratory, Pasadena, California. This work was supported by the Office of Basic Energy Sciences, Division of Chemical Sciences, U.S. Department of Energy. Mound is operated by Monsanto Research Corporation for the U.S. Department of Energy under Contract No. DE-AC04-76 DP00053.

*Present address: Magnetic Heads and Systems Division, Kodak Research Laboratories, 11633 Sorrento Valley Road, San Diego, CA 92121.

[1]T. K. Halstead, J. Solid State Chem. **11**, 114 (1974); T. K. Halstead, N. A. Abood, and K. H. J. Buschow, Solid State Commun. **19**, 425 (1976).

[2]R. G. Barnes, W. C. Harper, S. O. Nelson, D. K. Thome, D. R. Torgeson, J. Less-Common Met. **49**, 483 (1976).

[3]R. F. Karlicek, Jr. and I. J. Lowe, J. Less-Common Met. **73**, 219 (1980); R. F. Karlicek, Jr. and I. J. Lowe, Solid State Commun. **31**, 163 (1979); R. F. Karlicek, Jr., Ph.D. thesis, University of Pittsburgh, PA, 1979 (unpublished).

[4]R. C. Bowman, Jr., D. M. Gruen, and M. H. Mendelsohn, Solid State Commun. **32**, 501 (1979).

[5]R. C. Bowman, Jr., B. D. Craft, A. Attalla, M. H. Mendelsohn and D. M. Gruen, J. Less-Common Met. **73**, 227 (1980).

[6]A. Percheron-Guégan, C. Lartique, J. C. Achard, P. Germi, and F. Tasset, J. Less-Common Met. **74**, 1 (1980).

[7]P. Fischer, A. Furrer, G. Busch, and L. Schlapbach, Helv. Phys. Acta **50**, 421 (1977).

[8]A. F. Andresen, in *Hydrides for Energy Storage,* edited by A. F. Andresen and A. J. Maeland (Pergamon, Oxford, 1978), p. 61.

[9]V. V. Burnasheva, V. A. Yartys, N. V. Fadeeva, S. P. Solovev, and K. N. Semenenko, Dokl. Akad. Nauk SSSR **238**, 844 (1978).

[10]K. Niihara, Y. Katayama, and S. Yajima, Chem. Lett. (Chem. Soc. Japan), 613 (1973).

[11]Y. B. Kuz'ma and N. S. Bilonizhko, Kristallografiya **18**, 710 (1973).

[12]H. C. Siegmann, L. Schlapbach, and C. R. Brundle, Phys. Rev. Lett. **40**, 972 (1978).

[13](a) L. Schlapbach, A. Seiler, H. C. Siegmann, J. V. Waldkirch, P. Zurcher, and C. R. Brundle, in *Proceedings of the 2nd World Hydrogen Energy Conference, Zurich, 1978,* edited by T. N. Veziroglu and W. Siefritz (Pergamon, Oxford, 1979), p. 2637; (b) L. Schlapbach, J. Phys. F **40**, 2477 (1980).

[14]F. T. Parker and H. Oesterreicher, J. Less-Common Met. **79**, 297 (1981).

[15]R. C. Bowman, Jr. and W.-K. Rhim, J. Magn. Reson. **49**, 93 (1982).

[16]R. C. Bowman, Jr., Ph.D. thesis, California Institute of Technology, Pasadena, CA (1982), Chap. 2, available as U.S. DOE Report No. MLM-2999 from National Technical Information Service, U.S. Department of Commerce, 5285 Port Royal Road, Springfield, VA 22161.

[17]Y. B. Kuz'ma, N. S. Bilonizhko, and E. M. Nimkovich, Dopov. Akad. Nauk Ukr. RSR Ser. A **10**, 939 (1973).

[18]Y. B. Kuz'ma and M. P. Khaburskaya, Izv. Akad. Nauk SSSR, Neorg. Mater. **11**, (10), 1893 (1975).

[19]Y. B. Kuz'ma and N. S. Bilonizhko, Izv. Akad. Nauk SSSR, Neorg. Mater. **7**, (4), 620 (1971).

[20]C. S. Barrett and T. B. Massalski, *Structure of Metals,* 3rd ed. (McGraw-Hill, New York, 1966).

[21]J. F. Lynch and J. J. Reilly, J. Less-Common Met. **87**, 225 (1982).

[22]K. H. J. Buschow and H. H. van Mal, J. Less-Common Met. **29**, 203 (1972).

[23]J. A. Elton and H. Oesterreicher, Rev. Sci. Instrum. **54**, 1684 (1983).

[24]H. H. van Mal, Philips Res. Rep. Suppl. **1**, 1 (1976).

[25]R. M. Cotts, in *Hydrogen in Metals I,* edited by G. Alefeld and J. Volkl (Springer, Berlin, 1978), p. 227.

[26]D. G. Westlake, J. Less-Common Met. **91**, 1 (1983).

[27]H. Nowotny and P. Rogl, *Boron and Refractory Borides,* edited by V. I. Matkovich (Springer, Berlin, 1977), p. 413; B. Post, in *Boron, Metallo-Boron Compounds and Boranes,* edited by R. A. Adams (Interscience, New York, 1964), p. 301.

[28]N. Bloembergen, E. M. Purcell, and R. V. Pound, Phys. Rev. **73**, 679 (1948).

[29]R. M. Cotts, Ber. Bunsenges, Physk. Chem. **76**, 760 (1972).

[30]R. C. Bowman, Jr., in *Metal Hydrides,* edited by G. Bambakidis (Plenum, New York, 1981), p. 109.

[31]T.-T. Phua, R. G. Barnes, D. R. Torgeson, D. T. Peterson, M. Belhoul, and G. A. Styles, in *Electronic Structures and Properties of Hydrogen in Metals,* edited by P. Jena and C. B. Satterthwaite (Plenum, New York, 1983), p. 467; M. Belhoul, G. A. Styles, E. F. W. Seymour, T.-T. Phua, R. G. Barnes, D. R. Torgeson, and D. T. Peterson, J. Phys. F **12**, 2455 (1982); T.-T. Phua, B. J. Beaudry, D. T. Peterson, D. R. Torgeson, R. G. Barnes, M. Belhoul, G. A. Styles, and E. F. W. Seymour, Phys. Rev. B **28**, 6227 (1983).

[32]C. Korn and S. D. Goren, Phys. Rev. B **22**, 4727 (1980).

[33]C. Crowder, W. J. James, and W. Yelon, J. Appl. Phys. **53**, 2637 (1982).

[34]V. A. Yartys, V. V. Burnasheva, S. E. Tsirkunova, E. N. Kozlov, and K. N. Semenenko, Kristallografiya **27**, 242 (1982) [Sov. Phys.—Crystallogr. **27**, 148 (1982)]; V. A. Yartys, V. V. Burnasheva, K. N. Semenenko, N. V. Fadeeva, and S. P. Solov'ev, Int. J. Hydrogen Energy **7**, 957 (1982).

[35]J. C. Achard, A. J. Dianoux, C. Lartigue, A. Percheron-Guégan, and F. Tasset, in *The Rare Earths in Modern Science and Technology, Vol. 3,* edited by C. J. McCarthy, H. B. Silber, and J. J. Rhyne (Plenum, New York, 1982), p. 481.

[36]D. G. Westlake, J. Less-Common Met. **91**, 275 (1983).

[37]J. C. Achard, C. Lartigue, A. Percheron-Guégan, A. J. Dianoux, and F. Tasset, J. Less-Common Met. **88**, 89 (1982).

[38]D. Richter, R. Hempelmann, and L. A. Vinhas, J. Less-Common Met. **88**, 353 (1982).

[39]D. Noréus, L. G. Olsson, and P.-E. Werner, J. Phys. F **13**, 715 (1983).

[40]H. Chang, I. L. Lowe, and R. J. Karlicek, Jr., in *Nuclear and Electron Resonance Spectroscopies Applied to Materials Science,* edited by E. N. Kaufmann and G. K. Shenoy (Elsevier, Amsterdam, 1981), p. 331.

[41]T. C. Jones, T. K. Halstead, and K. H. J. Buschow, J. Less-Common Met. **73**, 209 (1980).

[42]R. C. Bowman, Jr., B. D. Craft, A. Attalla, and J. R. Johnson, Int. J. Hydrogen Energy **8**, 801 (1983).

[43]H. Chang, M. Engelsberg, and I. J. Lowe, Solid State Ionics **5**, 609 (1981).

[44]R. E. Walstedt, R. Rupree, J. P. Remeika, and A. Rodriguez, Phys. Rev. B **15**, 3442 (1977).

[45]R. L. Kleinberg and B. G. Silbernagel, Solid State Commun. **33**, 867 (1980).

[46]J. L. Bjorkstam and M. Villa, J. Phys. (Paris) **42**, 345 (1981).

[47]M. Polak and D. C. Ailion, J. Chem. Phys. **67**, 3029 (1977).

[48]H. T. Stokes, T. A. Case, D. C. Ailion, and C. H. Wang, J. Chem. Phys. **70**, 3563 (1979).

[49]P. Beckmann, Chem. Phys. **63**, 359 (1981).

[50]W. Muller-Warmuth and W. Otte, J. Chem. Phys. **72**, 1749 (1980).

[51]E. Göbel, W. Müller-Warmuth, H. Olyschlager, and H. Dutz, J. Magn. Reson. **36**, 371 (1979).

[52]A. Avogadro and M. Villa, J. Chem. Phys. **66**, 2359 (1977).

[53]C. A. Sholl, J. Phys. C **14**, 447 (1981).

[54]T. K. Halstead, K. Metcalfe, and T. C. Jones, J. Magn. Reson. **47**, 292 (1982).

[55]A. M. Albano, P. A. Beckmann, M. E. Carrington, F. A. Fusco, A. E. O'Neill, and M. E. Scott, J. Phys. C **16**, L979 (1983).
[56]J. E. Anderson, J. Magn. Reson. **11**, 398 (1973).
[57]P. A. Fedders, Phys. Rev. B **18**, 1055 (1978).
[58]A. Abragam, *Principles of Nuclear Magnetism* (Oxford University Press, London, 1961), p. 461.
[59]D. Wolf, Phys. Rev. B **10**, 2724 (1974); D. Wolf and P. Jung *ibid.* **12**, 3596 (1975).
[60]A. N. Garroway, J. Magn. Reson. **34**, 283 (1979).